

Short Communication

Study on the Synthesis and Electrochemical Properties of Cr-Sb Co-doped TiO₂

Min Zeng*, Hui Xu, Xiao-Hua Huang

School of Materials Science and Engineering, Southwest University of Science and Technology, Mianyang 621010, P R China

*E-mail: zengmin@swust.edu.cn

Received: 27 August 2015 / Accepted: 30 September 2015 / Published: 4 November 2015

Cr-Sb co-doped rutile Ti_{0.9}Cr_{0.05}Sb_{0.05}O₂ was synthesized using a traditional solid-state method. The properties of the samples were investigated using X-ray diffraction, Scanning Electron Microscopy, Energy-Dispersive Spectrometry, and UV-vis-NIR diffuse reflection spectroscopy. The UV-vis light photo-catalytic characterizations were studied, using methylene blue as an organic dye. The effects on the photoelectric performance of dye-sensitized solar cells (DSSCs) were characterized by current-voltage curve.

Keywords: Nanostructures; Semiconductors; Catalytic properties; Electrochemical properties

1. INTRODUCTION

Titanium dioxide has a wide range of industrial applications in a variety of areas, including photocatalysts, electronic ceramics, pigments, dye-sensitized solar cells and others [1-8]. However, the relatively large band gap of TiO₂ limits its ability to absorb ultraviolet (UV) light, which considerably limits the utilization of natural solar light [1]. Metal doping (such as Sb, Nb or W) has been reported to be an effective way to induce visible-light absorption [9-12]. As is well known, metal doping can form a localized state slightly above the valence band in the band gap of TiO₂, causing band narrowing, which is energetically favorable for enhancement of visible light absorption [12-13]. But this phenomenon requires further study to determine if the visible light absorption leads to a visible light photo-catalytic activity increase and a change in the photoanode property in DSSCs [5].

On the other hand, because Cr ions typically complete their diffusion in the rutile phase at about 750°C [9-12], the synthesis of Cr doped TiO₂ must be performed at a high temperature to ensure that the dopants are completely introduced into the rutile lattice and homogeneously dispersed into the rutile matrix, either during the solution processing or in a solid-state reaction. The solid-state reaction

is generally preferred in industrial production, because raw materials required for solution processing are quite expensive. In this reported study, Cr-Sb co-doped TiO₂ was synthesized to obtain new insight into the co-doping effect, by a solid-state reaction from 800 °C to 1300 °C. The UV-vis-NIR reflectance and band gap changes of the doped TiO₂ are also were discussed during the anatase-to-rutile transformation. The photo-catalytic results indicate that the Cr-Sb co-doped TiO₂ showed no visible light photo-catalytic activity and the 0.5% Ti_{0.9}Cr_{0.05}Sb_{0.05}O₂ photoanode-based DSSC achieved an improved conversion efficiency compared with a cell employing commercial P25-TiO₂ nanoparticles. This study may be relevant for the specific analyzed case, but may also introduce additional general useful concepts related to the co-doping of semiconductors for photocatalytic and photochemical purposes.

2. EXPERIMENTAL

The Cr-Sb co-doped TiO₂ was synthesized using a solid-state reaction [10-11]. Titanium dioxide (TiO₂), Cr₂O₃, Sb₂O₅ and combustion promoters NH₄NO₃, CaCO₃ were wet mixed in appropriate proportions and then milled in an agate mortar until homogenous [14]. The homogeneous mixtures were calcined at 1000 °C in an air atmosphere for 2 h with a thermal rate of 5 °C/min. As a control, the analytical reagent, rutile-TiO₂ was calcined at 1000 °C. All chemicals used were of analytical grade.

The photocatalytic reaction experiments of the prepared samples and controls were performed by analyzing the degradation of methylene blue (MB) in an aqueous solution [15]. For this purpose, a 254nm UV light was used and a 300W xenon light (simulated sunlight), with 400nm or 460nm LP-filters, plus a refrigerating water circuit was employed. The TiO₂ photoanodes of the DSSC were prepared on FTO glass substrates, treated with an aqueous solution of TiCl₄, and immersed into N719 ruthenium dye ethanol solution [5-6]. The sensitized photoelectrode and Pt counter electrode were fixed together using a hot-melt ionomer film. The gap between the electrodes was filled with a liquid electrolyte. To confirm the effect, the weight percentages of Ti_{0.9}Cr_{0.05}Sb_{0.05}O₂: P25-TiO₂ in the composite films was 0, 0.5, 1, 50 and 100wt%.

The microstructures of the products were observed by an X-ray diffraction analyzer (XRD), field emission scanning electron microscope (FE-SEM, Ultr55, Zeiss). The elemental compositions were determined with a Link ISIS energy dispersive X-ray spectrometer (EDS). The diffuse reflectance spectra were performed in the 200–1350 nm range using this spectrophotometer with an integrating sphere (Shimadzu UV-3150). The I-V characteristics of the DSSCs were measured using a Keithley 2612A source/meter under simulated sunlight (AM1.5, 100mWcm⁻², San-Ei).

3. RESULTS AND DISCUSSION

Fig.1 shows the XRD patterns of the samples: (a) P25-TiO₂, (b) TiO₂ calcined at 1000 °C, (c) Ti_{0.9}Cr_{0.05}Sb_{0.05}O₂, respectively. The pure rutile phase was obtained according to varying doping proportions, as shown in Fig.1(C). Neither Cr₂O₃ nor Sb₂O₅ were detected in the samples, even with

doping to 10wt%, which indicated that the Cr³⁺ ions and Sb⁵⁺ ions diffused completely into the rutile TiO₂ lattice [10]. In fact, because the ionic radius (r_{ion}) of Cr³⁺ and Sb⁵⁺ is larger than Ti⁴⁺, the XRD angle (2θ) decreased, indicating that the interplanar spacing increased, as shown in the inset of Fig.1.

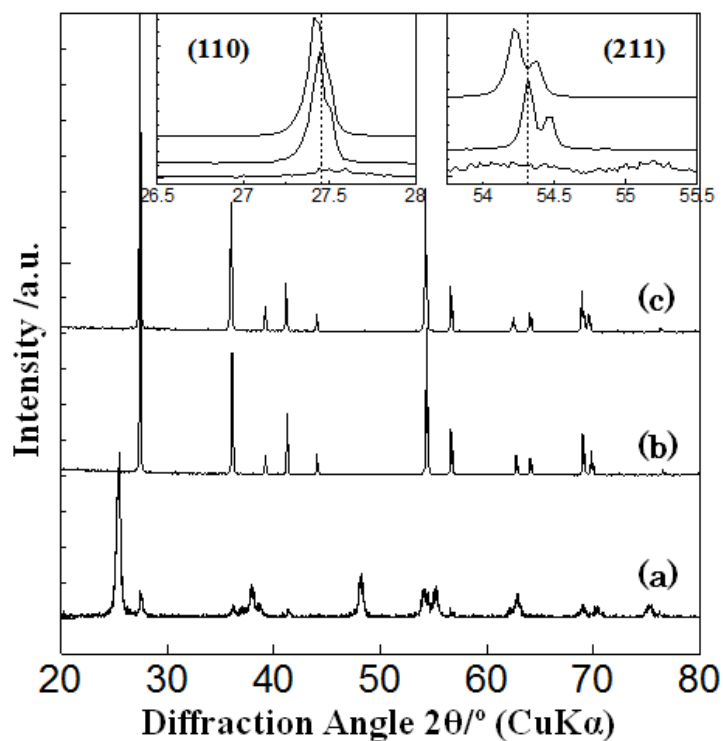


Figure 1. XRD patterns of the samples: (a) P25-TiO₂, (b) rutile TiO₂ (c) Ti_{0.9}Cr_{0.05}Sb_{0.05}O₂, respectively.

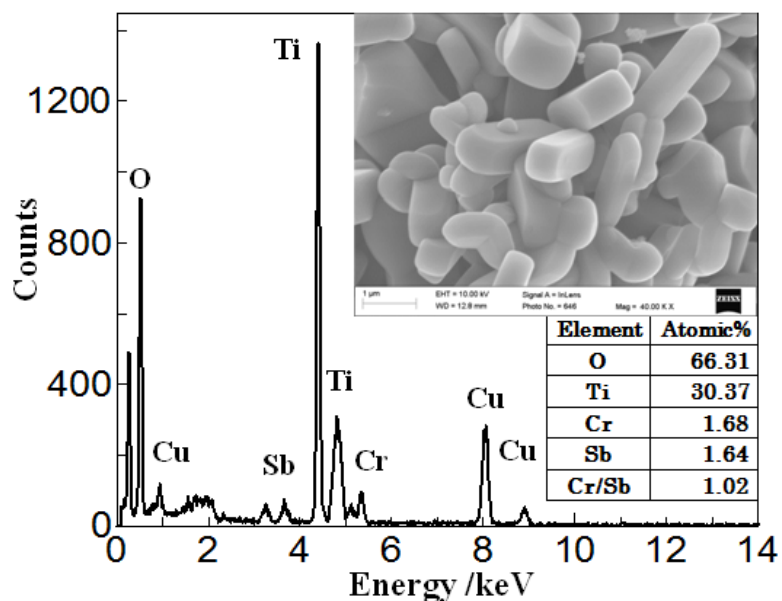


Figure 2. The SEM micrographs and EDS analysis of the Ti_{0.9}Cr_{0.05}Sb_{0.05}O₂ samples.

Figure 2 shows the SEM micrographs and EDS analysis of the samples. As shown in the SEM micrographs, the samples had narrow size distribution of $0.5\text{--}1\mu\text{m}$ and a regular geometric shape with clear surfaces, dispersed and homogeneous. The molar ratio of the samples analyzed by EDS is shown in Fig.2. The EDS patterns clearly indicate that, based on the Ti, Cr, Sb and O peaks, the final products were composed of $\text{Ti}_{0.91}\text{Cr}_{0.05}\text{Sb}_{0.049}\text{O}_{1.99}$, and the Cu peaks corresponded to a basilar plate. The presence of an oxygen vacancy also can be found and the slight deviation of the Cr/Sb molar ratios from 1 to 1.02 was due to the sublimation of Sb_2O_5 .

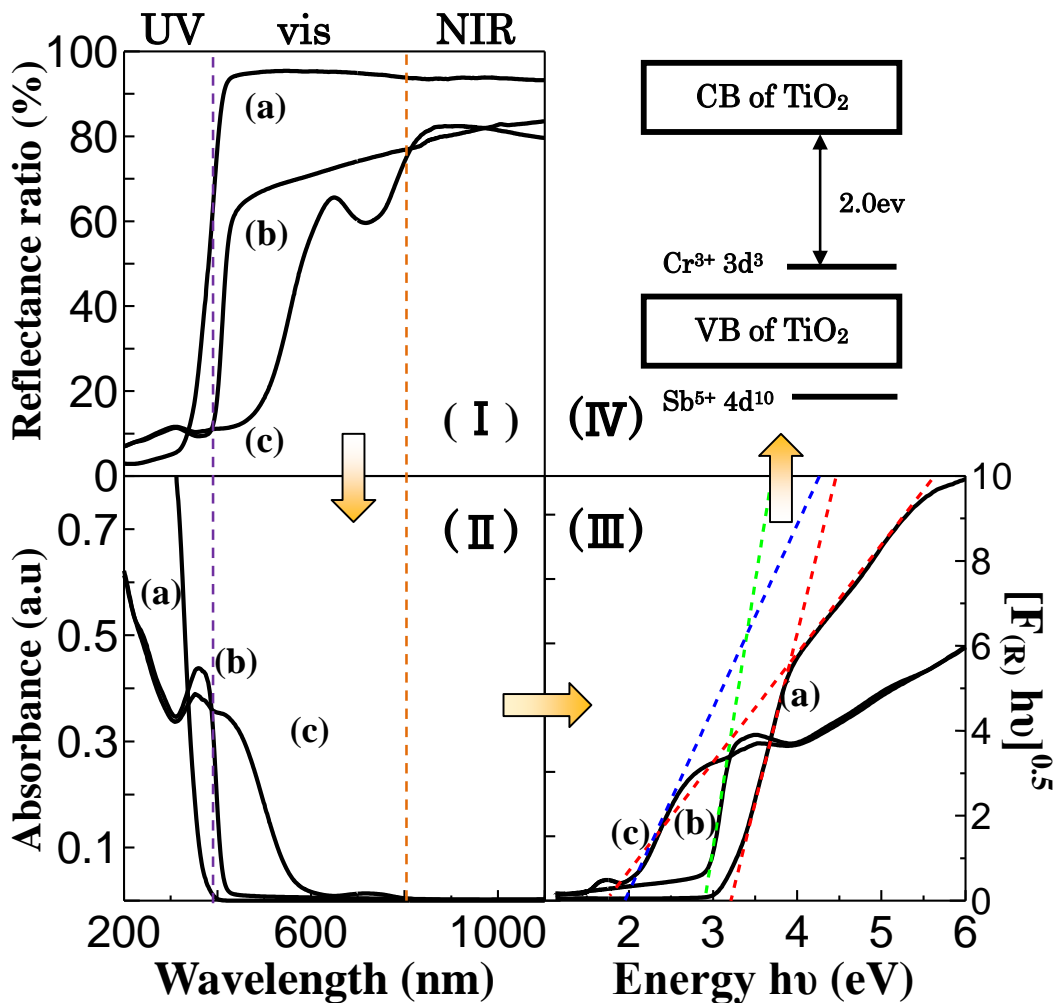


Figure 3. Optical spectra of the samples: (a) P25-TiO₂, (b) rutile TiO₂ (c) $\text{Ti}_{0.9}\text{Cr}_{0.05}\text{Sb}_{0.05}\text{O}_2$, respectively. (I): the UV-vis-NIR diffuse reflection spectra.(II): absorption spectra. (III): UV-vis reflection spectral changes and plot of $(\alpha/S)^{1/2}$ versus photo energy of samples with different. (IV): Proposed electronic states of $\text{Ti}_{0.9}\text{Cr}_{0.05}\text{Sb}_{0.05}\text{O}_2$.

The UV–Visible diffuse reflection spectra (I) and absorption spectra (II) of (a) P25-TiO₂, (b) rutile-TiO₂ calcined at 1000 °C and (c) $\text{Ti}_{0.9}\text{Cr}_{0.05}\text{Sb}_{0.05}\text{O}_2$, were recorded to evaluate their optical properties and band gap, as shown in Fig.3. The P25-TiO₂ and rutile-TiO₂ exhibited no absorption in the visible region. By contrast, the $\text{Ti}_{0.9}\text{Cr}_{0.05}\text{Sb}_{0.05}\text{O}_2$ showed an intense absorption band from 400nm

to 600nm, as exhibited in Fig.3(II). The band gaps were calculated and are shown in Fig.3(III) and are in accordance with [13]:

$$\alpha h\nu = B(h\nu - E_g)^n$$

where α is the absorption coefficient of the material (calculated from the absorption spectra), h is Plank's constant, ν is the frequency of the radiation, B is a constant (dependent on the nature of the material), E_g is the energy of the band gap, and n is a coefficient dependent on the type of transition considered (For direct transitions $n = 1/2$ [13]). As shown in Fig. 3(III), the direct band gaps of the P25-TiO₂ and rutile-TiO₂ were deduced to be at about 3.2eV and 3.0eV, according to the slope of the corresponding curves. However, the direct band gap of the Ti_{0.9}Cr_{0.05}Sb_{0.05}O₂ was found to be at around 2.0eV, which indicated that the donor level was prominent in the band gap [12, 16]. This confirms that a doping cation plays an important role for the absorption in the red-shifted bands. During our processing, chromium and antimony played an important role. Chromium, Cr³⁺ was expected to diffuse in the TiO₂ lattice and substitute for the Ti⁴⁺ sites in the octahedral coordination. With the embedded chromium ions, a donor level was found and absorption in the visible region became possible. Antimony, Sb⁵⁺ is thought to balance the mismatched charge between Ti⁴⁺ and Cr³⁺ to ensure the electroneutrality of the lattice [12, 16]. This means that a Cr/Sb co-doped TiO₂ should be characterized by fewer defects. Fig.3 (IV) shows the proposed electronic properties of TiO₂ doped with chromium and antimony.

The UV-vis photocatalytic activities of the samples were evaluated by the degradation of MB using a 254nm 30W UV lamp and a 300W Xenon lamp, as shown in Fig.4 (a, b). Under UV and Xenon lamp irradiation, the degradation rate of MB is more than 80% over 3 h using the P25 photocatalysts, whereas it is only 30% using rutile-TiO₂ and only 20% using Ti_{0.9}Cr_{0.05}Sb_{0.05}O₂. The differences can be ascribed to the crystal structures and the quantity of the adsorbed dyes.

To study the visible light photocatalytic activity and to ensure that the experiments were performed under suitable visible light, a Xenon lamp light beam was passed through a 400 nm long-pass optical filter or 460 nm LP filter, as shown in Fig.4(c, d). However, the degradation rate was found to be only 40% using P25, as shown in Fig.4(c). The degradation rate results for the other catalysts were also reduced, but not by as much. This phenomenon indicates that the Ti_{0.9}Cr_{0.05}Sb_{0.05}O₂ and rutile-TiO₂ have similar photo-catalyst activity. Fig. 4(d) shows that when use of a 460 nm LP filter, decreased the degradation rate to 0, which indicates that the Ti_{0.9}Cr_{0.05}Sb_{0.05}O₂ doesn't have any visible light photocatalytic activity. This is despite the fact that the absorption maxima λ_{\max} is about 620 nm. These results can be ascribed to the position of the valence and conductive bands in this material and the rate of the electron–hole recombination [2].

Fig.5 shows the photovoltaic performance and the corresponding photovoltaic parameters of the DSSCs based on various photoanodes. The typical DSSC using pure P25-TiO₂ as a photoanode possesses an absorption efficiency (FF) of 4.1% and a fill factor of 0.71. After doping TiO₂ with 0.5 wt% Ti_{0.9}Cr_{0.05}Sb_{0.05}O₂, the short-circuit current density decreased (J_{sc}) from 6.81 to 6.76 mAcm⁻², the efficiency increased to 4.2% and FF increased to 0.74 as shown in Fig.5(A) and (B). This suggests that the Ti_{0.9}Cr_{0.05}Sb_{0.05}O₂ acted as a charge-carrier pathway, reducing the charge recombination rate. These parameters show that the device performance was improved by insertion of small amounts of Ti_{0.9}Cr_{0.05}Sb_{0.05}O₂. On the other hand, doping with 1 wt% Ti_{0.9}Cr_{0.05}Sb_{0.05}O₂, caused the J_{sc} density to

decrease to 6.68 mAcm^{-2} , while the efficiency and FF significant decreased. Doping with 50 wt%, caused the J_{sc} to decrease to 2.41 mAcm^{-2} and the efficiency decreased to 1.3%. These results suggest that photoanodes have a large internal resistance, as shown in Fig. 5(C) and (D). Using pure $\text{Ti}_{0.9}\text{Cr}_{0.05}\text{Sb}_{0.05}\text{O}_2$ as photoanode does not have practical value, as shown in Fig. 5(E).

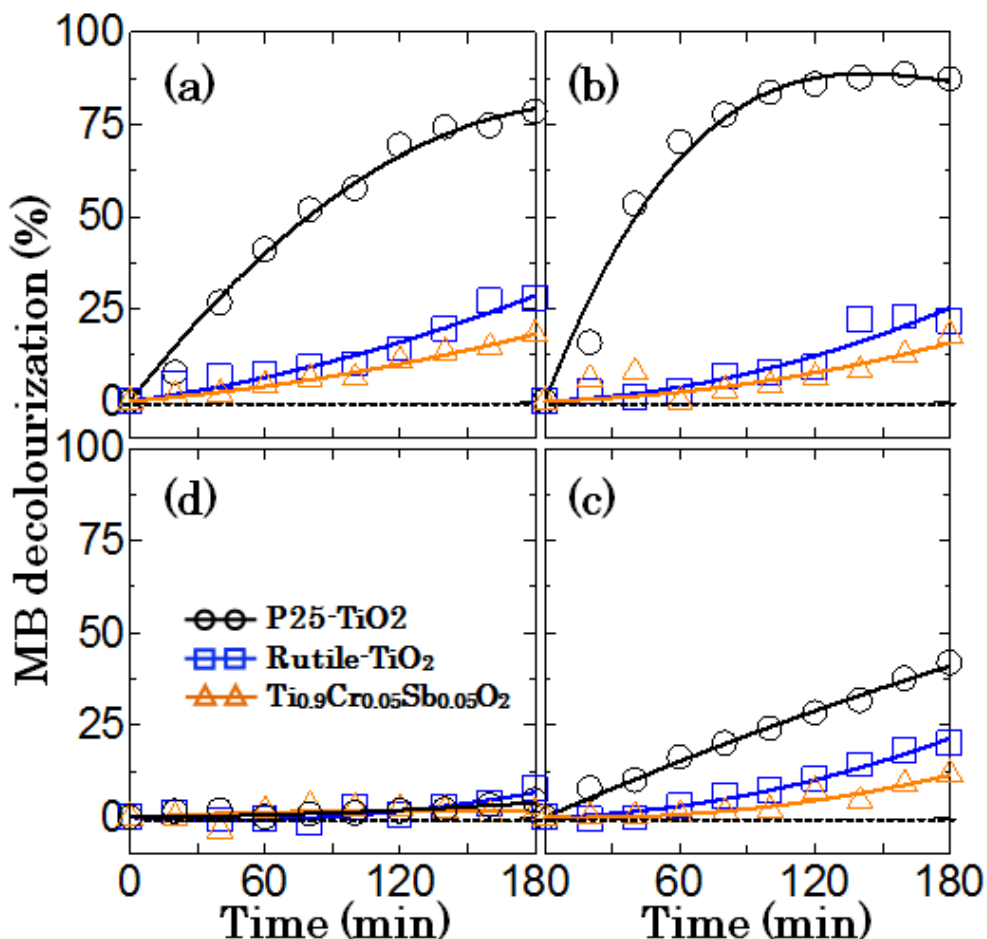


Figure 4. The degradation rate of methylene blue using: (a) 254nm UV lamp; (b) 300W Xenon lamp; (c) 300W Xenon lamp with 400nm LP filter or (d) with 460nm LP filter.

4. CONCLUSION

Cr^{3+} ions and Sb^{5+} successfully diffused into the rutile lattice and partly substituted for Ti^{4+} ions. The photo-catalytic results indicate that the $\text{Ti}_{0.9}\text{Cr}_{0.05}\text{Sb}_{0.05}\text{O}_2$ showed no visible light photo-catalytic activity, which was similar to rutile- TiO_2 . At a weight ratio 0.5% of $\text{Ti}_{0.9}\text{Cr}_{0.05}\text{Sb}_{0.05}\text{O}_2$ doped into P25- TiO_2 , the short-circuit current density and conversion efficiency of the DSSCs were higher than with pure TiO_2 , suggesting that the charge carriers of the retarded recombination improved the charge transfer.

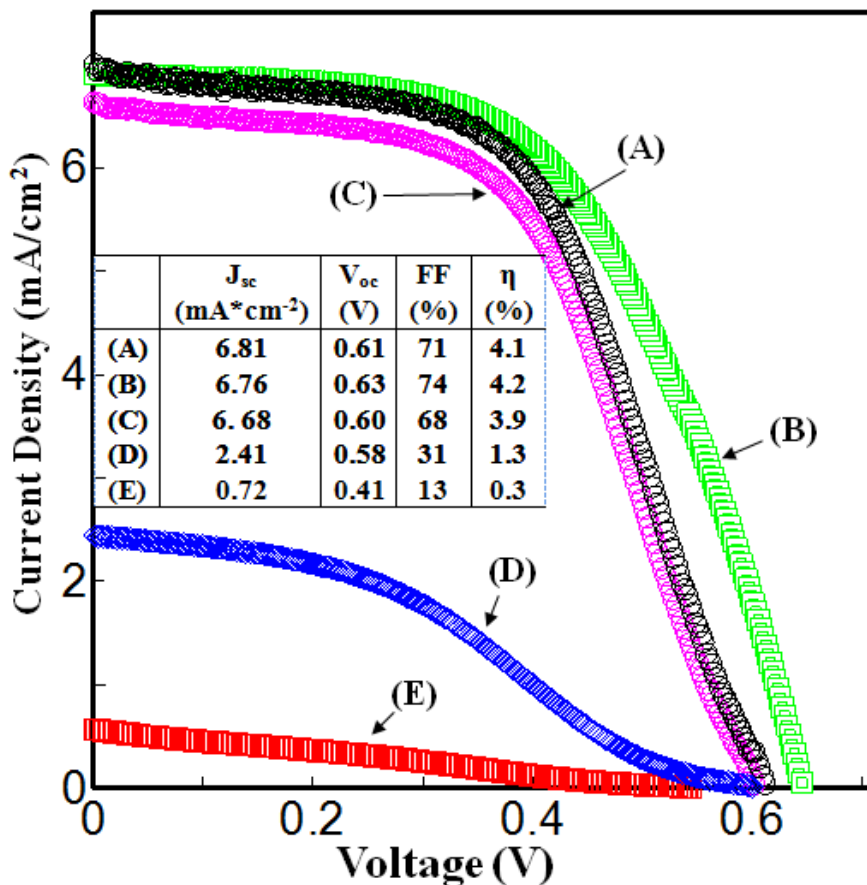


Figure 5. Photocurrent-voltage curves and Photovoltaic parameters (short-circuit current density, open-circuit voltage, fill factor, and efficiency) of DSSCs based on different photoanodes: (A): P25-TiO₂, (B): P25-TiO₂ with 0.5% rutile TiO₂, (C): P25-TiO₂ with 1% Ti_{0.9}Cr_{0.05}Sb_{0.05}O₂, (D): P25-TiO₂ with 50% Ti_{0.9}Cr_{0.05}Sb_{0.05}O₂, (E): Ti_{0.9}Cr_{0.05}Sb_{0.05}O₂, respectively.

References

- [1] D. Ulrike, *Surf. Sci. Rep.* 48 (2003) 53.
- [2] O. Carp, C.L. Huisman, A. Reller, *Prog. Solid. State. Chem.* 32 (2004) 33.
- [3] A. Libbra, L. Tarozzi, A. Muscio, M.A. Corticelli, *Opt. Laser. Technol.* 43 (2011) 394.
- [4] B. O'regan, M. Gratzel, *Nature*, 353 (1991) 737.
- [5] Z. Han, J. Zhang, W. Cao, *Mater. Lett.* 84 (2012) 34.
- [6] Y. Shi, L. Zhao, S.M. Wang, J. Li, B.H. Dong, Z.X. Xu, L. Wan, *Mater. Res. Bull.* 59 (2014) 370.
- [7] R.N. Mohammad, G. Maryam, B.M. Abdolmajid, D. Rassoul, S. Roya, *Int. J. Electrochem. Sci.*, 3 (2008) 1117.
- [8] S. Arman, H. N. Miankushki, *Int. J. Electrochem. Sci.*, 10 (2015) 3354.
- [9] Z. Jian, *Dyes. Pigm.* 97 (2013) 71.
- [10] T. Keda, T. Nomoto, K. Eda, Y. Mizutani, H. Kato, A. Kudo, H. Onishi, *J. Phys. Chem. C*, 112 (2008) 1167.
- [11] F.T.G. Vieira, D.S. Melo, S.J.G. Lima, E. Longo, C.A. Paskocimas, W.S. Júnior, *Mater. Res. Bull.* 44 (2009) 1086.
- [12] C.D. Valentin, G. Pacchioni, H. Onishi, A. Kudo, *Chem. Phys. Lett.* 469 (2009) 166.
- [13] D.M. Tobaldi, R.C. Pullar, A.S. Skapin, M.P. Seabra, J.A. Labrinch, *Mater. Res. Bull.* 50 (2014) 183.

- [14] X. H. Zuo, X. Y. Deng, Y. Chen, M. Ruan, W. Li, B. Liu, Y. Qu, B. Xu, *Mater. Lett.* 64 (2010) 1150.
- [15] H. Lachheb, E. Puzenat, A. Houas, M. Ksibi, E. Elaloui, C. Guillard, J. M. Herrmann, *Appl. Catal. B: Environ.*, 39 (2002) 75.
- [16] X. Yan, X. J. Huang, Y. Fang, Y. H. Min, Z. J. Wu, W. S. Li, J. M. Yuan, L. G. Tan, *Int. J. Electrochem. Sci.*, 9 (2014) 5155.

© 2015 The Authors. Published by ESG (www.electrochemsci.org). This article is an open access article distributed under the terms and conditions of the Creative Commons Attribution license (<http://creativecommons.org/licenses/by/4.0/>).